Published in final edited form as:
Dev Biol. 2009 October 1; 334(1): 97–108. doi:10.1016/j.ydbio.2009.07.021.

Stabilized β-catenin in lung epithelial cells changes cell fate and leads to tracheal & bronchial polyposis

Changgong Li[1,*], **Aimin Li**[1], **Min Li**[1], **Yiming Xing**[1], **Hongyan Chen**[1], **Lingyan Hu**[1], **Caterina Tiozzo**[1], **Stewart Anderson**[2], **Makoto Mark Taketo**[3], and **Parviz Minoo**[1]

[1]Department of Pediatrics, Women's & Children's Hospital, USC Keck School of Medicine, Los Angeles, CA90033

[2]Department of Psychiatry, Weill Medical College of Cornell University, New York, NY10021

[3]Department of Pharmacology, Kyoto University Graduate School of Medicine, Yosida Konoe-cho, Sakyo-ku, Kyoto 606-8501, Japan

Abstract

The precise mechanisms by which β-catenin controls morphogenesis and cell differentiation remain largely unknown. Using embryonic lung development as a model, we deleted exon 3 of β-catenin via *Nkx2.1-cre* in the *Catnb[+/lox(ex3)]* mice and studied its impact on epithelial morphogenesis. Robust selective accumulation of truncated, stabilized β-catenin was found in *Nkx2.1-cre; Catnb[+/lox(ex3)]* lungs that was associated with the formation of polyp-like structures in the trachea and main-stem bronchi. Characterization of polyps suggests that accumulated β-catenin impacts epithelial morphogenesis in at least two ways. "Intracellular" accumulation of β-catenin blocked differentiation of spatially-appropriate airway epithelial cell types, Clara cells, ciliated cells and basal cells, and activated UCHL1, a marker for pulmonary neuroendocrine cells. There was also evidence for a "paracrine" impact of β-catenin accumulation, potentially mediated via activation of Bmp4 that inhibited Clara and ciliated, but not basal cell differentiation. Thus, excess β-catenin can alter cell fate determination by both direct and paracrine mechanisms.

Keywords

β-catenin; stabilized; Wnt; Nkx2.1; UCHL1; polyposis; lung development; cell fate

Introduction

Wnt signaling plays important roles in many cellular activities in embryogenesis and adult tissue homeostasis (Ling et al., 2009; Logan and Nusse, 2004; van Amerongen and Berns, 2006). The activity of canonical Wnt signaling, also named Wnt/β-catenin signaling, is mediated by the stabilization of β-catenin. In the absence of Wnt ligands, β-catenin is phosphorylated on Ser 33, 37, 45 and Thr 41 by the APC/Axin/GSK3β complex. Phosphorylated β-catenin is ubiquitinated and degraded through the E3 ubiquitin ligase, β-

*Address correspondence to: Changgong Li, Ph.D., General Laboratories Building, 1801 E. Marengo Street, Room 1G1, Los Angeles, CA 90033, (323) 226-5040, (323) 226-5049 FAX, changgon@usc.edu

TrCP (Marikawa and Elinson, 1998). Upon binding to their receptor Frizzled (Fzd) and co-receptor Lrp5/6 on the cell membrane, the Wnt ligands trigger a series of intracellular responses that lead to inhibition of β-catenin phosphorylation. The stabilized β-catenin thus accumulates and translocates to the nucleus where it interacts with the LEF/TCF transcription factor complex to regulate target gene expression (Morin et al., 1997).

β-catenin is a non-redundant and central component of the canonical Wnt pathway. As such, it is an attractive target of genetic manipulations. Conventional deletion of β-catenin results in failure to form an embryonic anterior-posterior axis and leads to early lethality (Haegel et al., 1995). Conditional inactivation of β-catenin by multiple studies has revealed the important role of this molecule in morphogenesis of, and cellular differentiation in many tissues (Grigoryan et al., 2008). Some of the vital functions of β-catenin have been uncovered by conditional gain-of-function mutations. Genetic targeting of the phosphorylation-mediated mechanism of Wnt/β-catenin signaling can be used to generate conditional and tissue-specific gain-of function mutations. The region containing the GSK3β-mediated phosphorylation sites is encoded by exon 3 in the β-catenin gene. Deletion of exon 3 results in production and accumulation of a truncated but stabilized β-catenin protein that is resistant to the APC/Axin/GSK3β-mediated E3 ubiquitin ligase degradation (Harada et al., 1999). A genetically engineered mouse line, designated *Catnb[+/lox(ex3)]* has been generated in which exon 3 of β-catenin is floxed by two loxP sequences (Harada et al., 1999). When *Catnb[+/lox(ex3)]* were crossed to *CK19-cre* or *Fabpl-cre* mice that express a cre recombinase in the intestine, adenomatous intestinal polyps developed in early adulthood, associated with accumulation of stabilized β-catenin (Harada et al., 1999).

Embryonic lung development represents a useful model in which to study complex tissue interactions and cell differentiation in organ development. Lung development commences with outgrowth of an endodermally-derived lung primordium that eventually forms the primitive trachea and bronchi. The primitive bronchi undergo branching morphogenesis to form the architecture of the lung. During this process, the airway epithelial cells differentiate into distinct cell types, each performing a specialized function within the mature lung. The trachea and the main-stem bronchi are composed of three major cell types; the “ciliated”, “Clara” and, “basal” cells (Rawlins and Hogan, 2006). Pulmonary neuroendocrine cells (PNECs) are rare in the trachea, but more numerous in the intermediate and small airways as solitary cells and innervated clusters named neuroendocrine bodies (NEB). The distal airway epithelial cells differentiate around birth into alveolar type II (ATII) and alveolar type I (ATI) cells. Cell differentiation during lung morphogenesis is regulated by many factors including Wnt, Fgf, Shh and Bmp4 signaling.

Functional importance of Wnt signaling in lung morphogenesis has been analyzed by different approaches. The role of Wnt5a and Wnt7b were investigated by gene-targeting. We found that deletion of Wnt5a caused over-branching of the epithelial airway and thickening of the mesenchymal interstitium suggesting that Wnt5a regulates epithelial-mesenchymal interactions in the developing lung (Li et al., 2002). Targeted disruption of Wnt7b showed that it is required for activation of canonical Wnt signaling and proper lung mesenchymal growth and vascular development (Shu et al., 2002; Wang et al., 2005). Over-expression of the Wnt signaling inhibitor Dkk1 disrupted distal lung branching morphogenesis (Shu et al., 2005). Mutation of R-spondin 2, a ligand that activates Wnt/β-catenin signaling, caused lung hypoplasia and laryngeal-tracheal cartilage malformation (Bell et al., 2008).

Importance of β-catenin in lung development has also been examined. Conditional loss of β-catenin function in lung epithelial cells by *SpC-rtta;Teto-cre* system inhibited distal lung development (Mucenski et al., 2003). Deletion of β-catenin in lung mesenchymal cells caused multiple mesenchymal-related defects (De Langhe et al., 2008). Stabilization of β-catenin in

Clara cells disrupted lung morphogenesis (Mucenski et al., 2005) and expanded lung stem cell pools (Reynolds et al., 2008) whereas over-expression of a β-catenin-Lef1 fusion protein caused changes in endodermal cell fate determination (Okubo and Hogan, 2004).

The availability of a novel cre driver mouse line exploiting the regulatory elements of the earliest known marker of lung endodermal determination, the homeodomain gene Nkx2.1 presents the opportunity to investigate the role of early activation of β-catenin in lung morphogenesis and cell lineage determination. Accordingly, we generated and characterized lungs from *Nkx2.1-cre; Catnb[+/lox(ex3)]* mice. We found that stabilization of β-catenin leads to dilation of airways and formation of polyp-like structures in the trachea and main-stem bronchi. The epithelial cells with accumulated β-catenin fail to differentiate to ciliated, Clara, or basal cells, but express high levels of UCHL1, a marker of pulmonary neuroendocrine cells, indicating cell fate changes. These cells express high levels of Bmp4 and inhibit differentiation of adjacent epithelial cells toward ciliated or Clara cells.

Results

Phenotype of *Nkx2.1-cre;Catnb[+/lox(ex3)]* lungs

Activity of Nkx2.1-cre recombinase was detected in both proximal and distal epithelial airways by LacZ in *Nkx2.1-cre; Rosa26-LacZ* embryonic lungs. A complete pattern of Nkx2.1-cre activity in the lung was reported by Tiozzo et al (Manuscript submitted). *Nkx2.1-cre;Catnb [+/lox(ex3)]* fetuses, generated by crossing *Nkx2.1-cre* and *Catnb[+/lox(ex3)]* mice and simply referred to as *CatnbEx3(cko/+)* died perinatally. Although the cause of death remains unknown it may be related to non-structural defects in the lung or specific central nervous system lesions, as Nkx2.1-cre is also active in the latter tissue. *Nkx2.1-cre* mediated deletion of β-catenin exon 3 in *Nkx2.1-cre;Catnb[+/lox(ex3)]* lungs was verified by PCR analysis as shown in Figure 1 (panel B). Gross morphological examination of E18 lungs showed no detectable differences in the overall size and lobation of the *CatnbEx3(cko/+)* lungs, compared to controls (Figure 1, panels C & D). However, *CatnbEx3(cko/+)* lungs were characterized by a reproducible and consistent phenotype that included large, dilated airways especially in the anterior tip of left lobe (Figure 1, panels H-L). Abnormal cartilage formation was also discernible in the mutant trachea (Figure 1, panel F). In addition, structures resembling polyps were present in the lumen of the proximal airways including the trachea (Figure 1, panel G)

Histological characterization of E16 control and *CatnbEx3(cko/+)* lungs showed that dilation of distal airways occurred throughout the mutant lungs (Figure 2, panels E & I), with the most severe dilation detectable around anterior tip of the left lobe (asterisk, Figure 2, panel I). H&E staining of tissue sections of the polyp-like structures (referred to here simply as polyps) in the mutant main-stem bronchi (Figure 2, panel G) and trachea (Figure 2, panel H) revealed similar histological structures. Immunostaining with antibodies for epithelial and mesenchymal markers revealed that the core of polyps consists of masses of mesenchymal cells that express Vimentin, a marker of mesenchymal cell lineage (Figure 2, panel K) (Yamada et al., 2008). This mesenchymal cell mass is covered by a layer of Nkx2.1 expressing epithelial cells (Figure 2, panel L) that is contiguous with that of the normal appearing airway epithelium.

Selective accumulation of stabilized β-catenin

To determine whether deletion of exon 3 resulted in stabilization and accumulation of β-catenin, we performed immunofluorescent staining with an anti-β-catenin antibody. As shown in Figure 3, robust increase of β-catenin was observed in clusters of epithelial cells along the airways of *CatnbEx3(cko/+)* lungs (panels A & B). Surprisingly, accumulated β-catenin in the proximal lung was detectable exclusively in the cells that form the outer wall of the main-stem bronchi (Figure 3, panel A). This pattern is inconsistent and more spatially restricted, compared

to that of Nkx2.1-cre activity as assessed by LacZ in *Nkx2.1-cre; Rosa26-LacZ* lungs (Figure 3, panels E & F). We further examined recombination mediated by *Nkx2.1-cre* in an entirely different floxed mouse line. Mice carrying floxed alleles of the gene for Pten, phosphatase and tensin homolog, were crossed to *Nkx2.1-cre* mice and the double transgenic embryos were examined using an anti-Pten antibody to determine the frequency and pattern of cre-mediated deletion of Pten in lung epithelial cells. As shown in Figure 3 (panels G to I), Pten is uniformly expressed in the epithelial cells of E14 wild-type main-stem bronchi and lung. Recombination by *Nkx2.1-cre* within the floxed Pten loci occurred with high efficiency as evidenced by absence of Pten immunoreactivity in nearly all the epithelial cells of *Nkx2.1-cre;Pten(f/f)* main-stem bronchi (Figure 3, panels J & K) and distal airways (Figure 3, panel L). The discrepancy between the pattern of Nkx2.1-cre activity and β-catenin accumulation was further verified in the triple transgenic, *Nkx2.1-cre;Catnb[+/lox(ex3)];Rosa26-LacZ* lungs (Supplemental Fig. 1). Therefore, although the mechanism remains unknown, accumulation of stabilized β-catenin via *Nkx2.1-cre* appears to occur highly selectively in airway epithelial cells. The mRNA level for total β-catenin was also measured in *CatnbEx3(cko/+)* lungs. Section in situ hybridization revealed moderate levels of β-catenin mRNA in all epithelial cells lining the main-stem bronchi in wild-type lungs (Figure 4, panel A) and in the epithelial cells lining the non-polyp areas of *CatnbEx3(cko/+)* lungs (Figure 4, panels B&D). Increased total β-catenin mRNA, which may represent a response to increased accumulated β-catenin was detected in the polyp epithelial cells in *CatnbEx3(cko/+)* main-stem bronchi (Figure 4, panel B). This increase in β-catenin mRNA was also observed in tracheal polyps (Figure 4, panel D) and the pattern was identical to β-catenin protein accumulation (Figure 4, panel C). This result demonstrates that selective accumulation of β-catenin is accompanied by increased β-catenin mRNA.

To determine whether the wild-type or the stabilized forms of β-catenin accumulated in airway epithelial cells, we used immunofluorescent histochemistry with two anti-β-catenin antibodies (Figure 5). The antibody that recognizes both forms of β-catenin revealed that accumulation occurred specifically in the epithelial cells lining the apical surface of the polyps in *CatnbEx3 (cko/+)* main-stem bronchi (Figure 5C). An antibody specific to the N-terminal end of β-catenin (deleted in the stabilized form) did not show increased protein in the polyp's apical epithelium (Figure 5D). These observations indicate that it is the stabilized β-catenin, CatnbΔex3, that accumulates in the polyp epithelial cells.

Stabilized β-catenin is functional

To determine whether the accumulated β-catenin in *CatnbEx3(cko/+)* lungs is functionally active, we generated *Nkx2.1-cre; Catnb[+/lox(ex3)];TOPGAL*, triple transgenic mice. The *TOPGAL* transgenic mice exhibit LacZ (β-galactosidase) activity in response to activation of Wnt/β-catenin signaling (DasGupta and Fuchs, 1999). As shown in Figure 5 (panels E-J), LacZ activity is robustly increased in airways, especially in epithelium forming the polyps (arrows, Figure 5, panel H) in *Nkx2.1-cre; Catnb[+/lox(ex3)];TOPGAL* triple transgenic lungs. This suggests that from a functional standpoint, accumulation of β-catenin activates the Wnt/β-catenin signaling as assayed by TOPGAL activity.

Accumulation of stabilized β-catenin inhibits differentiation of ciliated, Clara, and basal cells

The function of the canonical Wnt signaling is closely associated with cell proliferation, cell fate determination and differentiation (Ling et al., 2009; Logan and Nusse, 2004; van Amerongen and Berns, 2006). Therefore, we examined whether the latter cellular properties were affected in the *CatnbEx3(cko/+)* lungs, especially in the epithelial cells forming the polyps. Immunostaining with Ki67 antibody revealed no significant differences in proliferation index between the epithelia of mutant and the control lungs (Figure 6, panel E).

Epithelial cell differentiation was examined using cell type-specific antibodies. An anti-α-tubulin antibody, a marker for the cilia of ciliated cells, showed normal distribution of these cells within the tracheal epithelium of wild type lungs (Figure 7, panel B). Similarly in the wild type lungs, distribution of CC10, a specific marker for Clara cells, was consistent with previous reports (Figures 7, panel C); (Rawlins and Hogan, 2006). In contrast, ciliated and Clara cells were identified only in the non-polyp epithelium of the trachea in the mutant lungs. Neither α-tubulin staining (Figure 7, panels E & K) nor CC10 staining (Figure 7, panels F & L) was found in the apical epithelial cells of the polyp-like structures. In the bronchioles, no α-tubulin staining or CC10 staining was observed in the epithelial cells with β-catenin accumulation (Figure 7, panels S & T). Another population of proximal airway epithelial cells is basal cell, which express the p53 family of transcription factors, p63. Basal cells are thought to act as progenitors of tracheal/airway epithelium (Hong et al., 2004; Rawlins and Hogan, 2006). Immunostaining with p63 antibody revealed no basal cells in the apical domain of the polyps where β-catenin is accumulated (Figure 8, panels D). Thus, accumulation of stabilized β-catenin within the apical domain of the polyp epithelium blocks cell differentiation along any of the three potential, ciliated, Clara or basal cell phenotypes.

As shown in Figure 7 (panel D), there are two epithelial domains in each polyp. The “apical domain” (boxed area, Figure 6, panel D) is composed of epithelial cells with robust accumulation of stabilized β-catenin. The “stalk domain” (bracket, Figure 6, panel D) is formed by epithelial cells that are contiguous with the airway epithelium and do not accumulate high levels of β-catenin. In addition to the apical domain, we also examined epithelial cell differentiation in the stalk domain.

Interestingly, in the epithelium of the polyp stalk domain where excess CatnbΔex3 does not accumulate, differentiation of ciliated and Clara cells was also inhibited (Figure 7, panels E, F, N & O), whereas that of basal cells was not. As shown in Figures 8, proximal epithelium along wild-type trachea or non-polyp areas of *CatnbEx3(cko/+)* trachea is composed of a layer of epithelial cells (ciliated and Clara cells) underlined by a layer of p63 positive basal cells. In contrast, the epithelium of the stalk domain adjacent to the apical domain of the polyps is clearly abnormal, consisting of one layer of epithelial cells, many of which are p63 positive (bracket, Figure 8, panel H). This observation raises the possibility of cross-communication via a paracrine mechanism between the polyp apical domain epithelial cells (arrows, Figure 8, panel G) and the epithelial cells within the stalk (boxed area, Figure 8, panel G).

Ectopic expression of Bmp4 in polyp epithelial cells

The latter observation (Figures 7&8) suggested the possibility that polyp apical epithelial cells which accumulate CatnbΔex3 may communicate with and inhibit differentiation of the adjacent epithelial cells (stalk domain, boxed in Figure 8, panel G). To understand the potential mechanism that mediates this interaction, we used in situ hybridization to examine the expression of Bmp4 (Figure 9). Weaver et al and Lu et al reported that Bmp4 signaling negatively regulates proximal epithelial cell differentiation (Lu et al., 2001;Weaver et al., 1999). As expected, in control lungs, Bmp4 was not detected in the epithelial cells lining the proximal airways or trachea (Figure 9, panels A & B), but was highly and specifically expressed in the epithelial cells at the tip of the distal buds (Figure 9, panel A). Interestingly, in *CatnbEx3 (cko/+)* lungs, abundant Bmp4 mRNA was detectable in the polyp apical epithelium as well as in the distal airways (Figure 9, panels D & E). Since Bmp4 expression in the distal epithelial cells is thought to be induced by Fgf10 signaling from the surrounding mesenchyme (Weaver et al., 2000), we also determined levels of Fgf10 mRNA. As shown in Figure 9 (panels C & F), Fgf10 mRNA level was not increased within the polyps in the *CatnbEx3(cko/+)* trachea, compared to the controls.

Accumulation of stabilized β-catenin stimulates expression of UCHL1, a marker for pulmonary neuroendocrine cells, PNECs

To investigate whether the polyp epithelial cells express any differentiated characteristics, we examined multiple markers of lung epithelial cell differentiation. One of these was ubiquitin carboxyl-terminal esterase L1 (UCHL1 or PGP9.5), which has been used as a marker for pulmonary neuroendocrine cells, PNECs, but also expressed by lung early neoplasm with neuroendocrine features (Brouns et al., 2008; Carolan et al., 2006; Poulsen et al., 2008). In wild-type lungs, UCHL1 is specifically expressed in PNECs localized within neuroendocrine bodies, NEBs, along the bronchi and bronchioles (Figure 10, panel B, inset). UCHL1 is weakly detectable in the epithelial layer of wild-type trachea. However, UCHL1 is strongly expressed in tracheal polyp epithelial cells where β-catenin is accumulated (Figure 10, panels D-F). Western blot analysis validated the immunofluorescent results (Figure 10, panel G). Furthermore, quantitative PCR revealed UCHL1 mRNA was significantly increased in mutant lungs compared to control (Figure 10, panel H).). In contrast to UCHL1, synaptophysin (SYP), a membrane protein of synaptic vesicles found in neurons, neuroendocrine cells and neuroendocrine neoplasm, was not expressed in polyp epithelial cells of the mutant lungs (Supplemental Fig. 2).

Discussion

The purpose of this study was to examine the consequences of epithelial-specific stabilization and accumulation of β-catenin on lung morphogenesis and cell differentiation. To this end, we used the cre-loxP system to permanently remove the floxed exon 3 of β-catenin thus resulting in accumulation of CatnbΔex3 protein, which lacks the N-terminal phosphorylation sites required for β-catenin degradation (Harada et al., 1999). We generated *CatnbEx3(cko/+)* double transgenic mice by mating between *Catnb[+/lox(ex3)]* mice and *Nkx2.1-cre* mice (Xing et al., 2008; Xu et al., 2008). Accumulation of CatnbΔex3 in the lung epithelial cells was accompanied by increased β-catenin mRNA. Morphologically, accumulation of CatnbΔex3 led to dilation of airways in the lung and formation of polyp-like structures in the proximal airways including trachea and main-stem bronchi. Functionally, accumulation of CatnbΔex3 led to cell fate changes as evidenced by, 1) inhibition of ciliated, Clara and basal cell differentiation, and 2) activation of UCHL1, a marker of pulmonary neuroendocrine cells. Cell differentiation was also inhibited in epithelial cells that lacked, but were adjacent to those with CatnbΔex3 accumulation. As the sites of CatnbΔex3 accumulation overlap with high level expression of Bmp4, we propose that inhibition of cell differentiation in these sites occurs via paracrine Bmp4 signaling.

To generate epithelial-specific gain-of-function mutation for β-catenin we used a novel cre mouse line in which expression of the recombinase is under the control of the Nkx2.1 regulatory elements. Nkx2.1 is a homeodomain transcription factor and the earliest known marker of lung endodermal determination. Activity of Nkx2.1-cre was detected in epithelial airways of embryonic lungs from as early as E10.5 (Tiozzo et al., Manuscript submitted). Thus, Nkx2.1-cre provides the opportunity for investigating the role of early activation of β-catenin in lung morphogenesis and cell lineage determination. A surprising finding of the current study is that stabilization of β-Catenin in epithelial cells occurred in a selective, rather than uniform manner in *CatnbEx3(cko/+)* lungs. For example, CatnbΔex3 protein accumulated in epithelial cells of the outer wall, but not the inner wall of the main-stem bronchi. It is unlikely that the selective pattern of β-catenin accumulation observed in the mutant lungs is due to Nkx2.1-cre selectivity (Figure 3). Whether the cells permissive to accumulation possess mechanisms that's lacking in those without accumulation remains unknown. Alternatively, the inner wall epithelial cells may have a mechanism that degrades truncated β-catenin via an exon3-independent pathway. Cell-type selective stabilization of β-catenin was also observed in early embryogenesis. Using

a *zona pellucida3-cre (Zp3-cre)*, Kemler et al expressed the CatnbΔex3 in developing oocytes (Kemler et al., 2004). CatnbΔex3 was not stabilized in pre-implantation embryos, but stabilized in early postimplantation embryos and led to premature cell fate changes in the embryonic ectoderm (Kemler et al., 2004). Detailed mechanism underlying cell specificity is unknown. Several GSK3β-independent β-catenin degradation mechanisms have been reported. For example, ubiquitin ligase Siah-1 and Siah-2, the mammalian homolog of *Drosophila seven in absentia*, degrade β-catenin independently of the GSK3β pathway (Liu et al., 2001;Matsuzawa and Reed, 2001;Topol et al., 2003). Also, the Gq pathway triggers calpain-mediated proteolysis of β-catenin in the human colon cancer cell line, SW480, independent of GSK3β (Li and Iyengar, 2002). Finally, although its relationship to GSK3β pathway remains unknown, Smad7, an antagonist for TGFβsignaling also induces β-catenin degradation through Smurf2 in keratinocytes (Han et al., 2006).

Another finding was increased mRNA for β-catenin in *CatnbEx3(cko/+)* lungs. Gain-of-function mutation generated by removal of exon 3 from β-catenin is thought to result in accumulation of available β-catenin simply by stabilization of the protein. In *CatnbEx3(cko/+)* lungs, we found not only a robust increase in β-catenin protein, but also mRNA (Figure 4). The mechanism for increased mRNA remains unknown, but as β-catenin is a target of Wnt signaling, it may potentially represent auto-regulation of β-catenin transcription by the stabilized protein. In support of this possibility, increased β-catenin mRNA has been observed in several intestinal-type gastric cancers with APC mutations (Ebert et al., 2002). Therefore, robust accumulation of β-catenin in the *CatnbEx3(cko/+)* lungs may be established by combined effects of stabilization of β-catenin protein as well as increased steady state level of β-catenin mRNA.

Stabilization and accumulation of β-catenin in lung epithelial cells caused both structural and cell fate changes in *CatnbEx3(cko/+)* lungs. Structural changes consisted of abnormal cartilage formation in the trachea and large, dilated airways especially in the anterior tip of the left lobe (Figures 1 & 2). The latter dilated airway phenotype was also found in gain-of-function mutations generated by Dox-regulated CCSP-rtTA;$(tetO)_7$-CMV-cre (Mucenski et al., 2005). However, the Nkx2.1-cre generated *CatnbEx3(cko/+)* lungs, also included structures resembling polyps which were not reported by previous studies (Mucenski et al., 2005;Okubo and Hogan, 2004;Reynolds et al., 2008). Intestinal polyposis is commonplace and thought to be precursor of colorectal cancer (Harada et al., 1999;Morin et al., 1997;Morson, 1974). Mutations of Wnt signaling mediators including APC, β-catenin and Axin are found in colorectal cancers (Fearnhead et al., 2005;Kolligs et al., 2002). Epithelial-specific stabilization of β-catenin in the intestine of transgenic *Catnb[+/lox(ex3)]* mice causes intestinal adenomas (Harada et al., 1999). In contrast, the formation of polyps in the lung is uncommon and a novel finding of the present study. The tracheal and bronchial “polyps” differ from intestinal polyps in the following aspects. First, unlike their intestinal counterparts which are composed solely of epithelial cells, the tracheal and bronchial polyps in *CatnbEx3(cko/+)* lungs consist of a mesenchymal core covered by an epithelium that is contiguous with the bronchial epithelial wall. Second, cell proliferation is not increased in tracheal and bronchial “polyps”, but is increased in intestinal polyps (Harada et al., 1999). This suggests that the lung polyps are unlikely to advance to tumors. However, as the *CatnbEx3(cko/+)* mice do not survive postnatally, this issue requires further experimentation. In several tissues such as liver, hyperactive Wnt signaling alone is not sufficient for tumorigenesis and may require additional genetic or epigenetic changes (Harada et al., 2002). Clinical report on tracheal polyposis is limited and its mechanism remains unknown (Fein et al., 1982). The *CatnbEx3(cko/+)* lung provides a useful in vivo model for studying tracheal and bronchial polyposis as well as the function of Wnt/β-catenin signaling in epithelial cell lineage specification.

In the mutant lungs, CatnbΔex3 accumulation is associated with ectopic Bmp4 expression in the apical epithelium of the polyps. It was reported previously that expression of Bmp4 is activated by Wnt/β-catenin signaling (Haegele et al., 2003). Whether Bmp4 has a role in polyp formation in the *CatnbEx3(cko/+)* lungs remains to be investigated. Several previous studies have demonstrated that BMP4 inhibits epithelial cell proliferation. For example, over-expression of BMP4 by SpC promoter results in reduced epithelial cell proliferation during lung morphogenesis (Bellusci et al., 1996). Similarly, recombinant BMP4 protein inhibits proliferation of cultured epithelial explants (Hyatt et al., 2002; Weaver et al., 2000). Therefore, high levels of BMP4 in epithelial cells with accumulated β-catenin may be the reason for a lack of proliferation in these epithelial cells.

Stabilization and accumulation of β-catenin in epithelial cells of *CatnbEx3(cko/+)* lungs also caused abnormalities in cell fate and differentiation. Careful characterization of cells particularly in regions of high CatnbΔex3 accumulation revealed that the impact of excess β-catenin on epithelial cell differentiation and cell fate can occur via at least two mechanisms.

First, stabilization of β-catenin and subsequent activation of Wnt signaling (Figure 5) may lead to cell fate changes in embryonic lung epithelial cells. This conclusion is based on the observation that expression of CatnbΔex3 in the lung epithelium resulted in inhibition of Clara, ciliated and basal cell differentiation (Figures 7 & 8). In addition, UCHL1, a marker of PNEC was found to be ectopically expressed in the epithelial cells where CatnbΔex3 accumulated. We propose that the latter changes are either direct consequences of excess intracellular β-catenin or secondary to its paracrine effects (please see below). In support of this proposal, level of β-catenin in PNECs of wild-type lungs is indeed higher than other epithelial cells along the airway (Figure 10). However, unlike a previous report (Okubo and Hogan, 2004) we found that robust accumulation of CatnbΔex3 had no impact on Nkx2.1, a transcription factor that is expressed in epithelial progenitor cells early in lung development, suggesting maintenance of lung epithelial cell identity (Figure 2). Furthermore, TTF3, a marker for intestinal cells, was clearly absent from either wild-type or *CatnbEx3(cko/+)* lungs (data not shown). These inconsistent results may simply reflect the inherent functional differences between CatnbΔex3 and β-catenin-Lef1 that was used in Okubo and Hogan's report.

Second, we found that differentiation of Clara and ciliated cells was also blocked in the epithelium that lacked robust expression of CatnbΔex3 but was adjacent to the polyps. The robust accumulation of CatnbΔex3 overlaps high level expression of Bmp4 (Figure 9). The function of BMP4 in inhibiting proximal airway epithelial cell differentiation has been demonstrated by both in vivo and in vitro studies. Bmp4 signaling negatively regulates proximal epithelial cell differentiation in transgenic animals that over-express BMP4 inhibitors (Lu et al., 2001;Weaver et al., 1999). Tracheal epithelial cells cultured in Matrigel differentiate and express CCSP (CC10) and HFH4 (Foxj1) in presence of FGF1. BMP4 inhibits the latter process and the BMP4 inhibitor, Noggin, blocks the inhibitory effect of BMP4 (Hyatt et al., 2002). Expression of Bmp4 is activated by Wnt/β-catenin signaling (Haegele et al., 2003). Thus, it is possible that accumulation of stabilized β-catenin stimulates Bmp4 expression thereby inhibiting Clara and ciliated cell differentiation in the adjacent epithelium. This is the paracrine mechanism of excess β-catenin effect on cell differentiation (Figure 11, Model). It is noteworthy that basal cell differentiation, as assessed by p63 expression was not blocked by high level of Bmp4 signaling in the adjacent cells (Figure 8), whereas it was blocked in cells with direct accumulation of CatnbΔex3. Therefore, differentiation of ciliated, Clara and basal cells may be differentially regulated by mechanisms involving Wnt/β-catenin and Bmp4 signaling.

In summary, stabilization of β-catenin in the lung epithelium occurs in a non-uniform pattern suggesting potential differences amongst epithelial cells that hitherto had been thought to be

of similar or identical developmental history. Excess β-catenin has both direct and paracrine effects on cell fate determination and differentiation. Finally, β-catenin gain-of-function using the cre-loxP system reflects both increased protein as well as mRNA. These observations should help elucidate the functional role of Wnt/β-catenin signaling during mammalian development.

Supplementary Material

Refer to Web version on PubMed Central for supplementary material.

Acknowledgements

We thank Dr. Brigid L. M. Hogan for Bmp4 cDNA. We thank Ben Lopes for the technical help. Supported by NHLBI grants HL075334 (Li), HL56590 & HL60231 (Minoo), and the Hastings Foundation.

Appendix

Appendix

Materials and methods

Mouse Breeding and Genotyping

All animals were maintained and housed in pathogen-free conditions according to the protocol approved by The University of Southern California Institutional Animal Care and Use Committee (IACUC) (Los Angeles, CA, USA).

The *Nkx2.1-cre* transgenic mouse was generated by pronuclear injection of a BAC clone carrying the Nkx2.1 gene, in which 15 bps of the second exon is replaced by the Cre recombinase (Xu et al., 2008).

Nkx2.1-cre; Catnb[+/lox(ex3)] mice were generated by breeding *Nkx2.1-cre* mice with *Catnb [+/lox(ex3)]* mice. Genotyping of the transgenic mice were determined by PCR with genomic DNA isolated from mouse tails or embryo tissue as described (Hogan, 1994). The forward (F) and reverse primers (R) for transgenic mouse genotyping are listed below.

β-*catenin*: (catnbF) 5′-CAT TGC GTG GAC AAT GGC TAC TCA-3′ and (catnbR1) 5′-CTA AGC TTG GCT GGA CGT AAA CTC-3′ for mutant, (catnbR2) 5′-GGC AAG TTC CGC GTC ATC C -3′ for Wild-type; *Nkx2.1-cre*: (creF) 5′-TAA AGA TAT CTC ACG TAC TGA CGG TG-3′ and (creR) 5′-TCT CTG ACC AGA GTC ATC CTT AGC-3′; TOPGAL: (Forward) 5′-ATC CTC TGC ATG GTC AGG TC-3′ and (Reverse) 5′-CGT GGC CTG ATT CAT TCC-3′.

Realtime Polymerase Chain Reaction (qPCR)

Quantification of selected genes by Realtime PCR was performed using a LightCycler (Roche Applied Sciences, IN) as previously described (Li et al., 2005). In brief, optimal PCR conditions for all investigated genes were established using the LightCycler Fast Start DNA Master SYBR Green I Kit (Roche Applied Sciences, IN). PCR products were checked by agarose gel electrophoresis for a single band of the expected size. A relative quantification analysis on a single channel experiment was carried out. The analysis uses the sample's crossing point, the efficiency of the reaction (specified as efficiency value of 2), the number of cycles completed, and other values to compare the samples and generate the ratios. Two ratios were compared: the ratio of a target gene to a reference gene (ß-actin or TBP) in samples of mutant lungs, to the ratio of the same two genes in samples of control lungs served as "Calibrator". The results

were expressed as a normalized ratio. All primers for qPCR were designed by using the program of Universal ProbeLibrary Assay Design Center from Roche Applied Sciences (IN).

Western Blot

Protein extracts were prepared from cultured cells and embryonic lungs with RIPA buffer (Sigma, MO) and separated on 7% SDS-PAGE gels. Proteins were then blotted to the Immobilon-P transfer membrane (Millipore Corp.). The membranes were analyzed with the ECL Western blot analysis system as described by the manufacturer (Amersham Biosciences, PA). In brief, the blotted membrane was blocked in 5% milk and then incubated with the primary antibody. Horseradish peroxidase-conjugated secondary antibody was used to detect the bound primary antibody. The membrane were then incubated in ECL reagents and exposed to Hyperfilm ECL.

In Situ Hybridization

Embryonic lungs were fixed in 4% paraformaldehyde, dehydrated, and then embedded in paraffin. Five to seven micrometer tissue sections were hydrated, pretreated with proteinase K and hybridized with Digoxigenin-labeled anti-sense RNA probe. After hybridization the sections were washed and treated with anti-Digoxigenin alkaline phosphatase (AP) conjugate. Color development was performed in the presence of NBT and BCIP. RNA anti-sense probes were prepared with Digoxigenin as label from following cDNAs. β-catenin: a 338 bp cDNA fragment of mouse β-*catenin* 3′-UTR cloned by PCR amplification; Fgf10: a 0.6-kb PCR product of the Fgf10 coding region. The probe for Bmp4 was a 1.5-kb Bmp4 cDNA (Kindly provided by Dr. Brigid L. M. Hogan, Duke University).

Immunohistochemistry and Immunofluorescent staining

Five-micrometer (um) tissue sections were prepared. Subsequent to deparaffinization, the sections were hydrated, heated in 10mM citrate buffer (pH6.0), treated with 1% H2O2 in methanol for 10 min and blocked with 10% of normal serum. The sections were then incubated with primary antibodies at 4°C overnight.

For immunohistochemistry staining, biotinylated secondary antibody and streptavidin-peroxidase conjugate (Zymed Laboratory, Inc.) were used to detect the bound antibodies.

For immunofluorescent staining, after normal serum blocking, the sections were incubated with a mixture of mouse monoclonal and rabbit or goat polyclonal antibody at 4°C for overnight. FITC-conjugated donkey anti-mouse IgG and Cy3-conjugated donkey anti-rabbit or anti-goat (Vector Laboratories) were applied for 1 hr at room temperature. Sections were preserved in VECTASHELD mounting medium with DAPI (to visualize nuclei).

Primary antibodies used are: mouse anti β-catenin (Transduction Laboratories, KY); rabbit anti-β-catenin (Anaspec, Inc); mouse anti-NKX2.1 & rabbit anti-Ki67 (Lab Vision, CA); mouse anti-p63 (BioGenex, CA); rabbit anti-UCHL1 & rabbit anti-α-tubulin (Abcam, MA); CC10 (Santa Cruz,CA); mouse anti-Vimentin (Sigma); mouse anti-SYP (Millipore, MA); rabbit anti-pro SpC (Seven Hills Bioreagents, OH).

LacZ (β-galactosidase) Staining

Activity of the β-galactosidase in embryonic lungs was determined by X-gal staining as described (Sanes et al., 1986). Briefly, E13 embryonic lungs were dissected, rinsed briefly, and fixed in 4% paraformaldehyde (PFA) for 15 minutes at 4°C. The tissues were then rinsed 3 times in Phosphate Buffered Saline (PBS), and stained overnight at room temperature in X-gal solution. Subsequent to staining the tissues were washed 3 times in PBS and stored in 4%

PFA. For histological study the tissues were dehydrated in ascending ethanol, embedded in paraffin and sectioned for analysis.

Proliferation assay

Proliferating cells in control or mutant lung sections were labeled with Ki67 antibody and the nuclei were counterstained with Hematoxylin. The sections were then photomicrographed. The labeled cells as well as the total number of epithelial cells along the proximal airways, photomicrographed at 40x, were counted. Ratio of proliferating cells in about 300 epithelial cells was calculated. The average ratio was then calculated from at least 6 ratios for each tissue. Significance of the difference in proliferation ratios between control and mutant proximal airway epithelial cells was determined by Student's t test.

References

Bell SM, Schreiner CM, Wert SE, Mucenski ML, Scott WJ, Whitsett JA. R-spondin 2 is required for normal laryngeal-tracheal, lung and limb morphogenesis. Development 2008;135:1049–1058. [PubMed: 18256198]

Bellusci S, Henderson R, Winnier G, Oikawa T, Hogan BL. Evidence from normal expression and targeted misexpression that bone morphogenetic protein (Bmp-4) plays a role in mouse embryonic lung morphogenesis. Development 1996;122:1693–1702. [PubMed: 8674409]

Brouns I, Oztay F, Pintelon I, De Proost I, Lembrechts R, Timmermans JP, Adriaensen D. Neurochemical pattern of the complex innervation of neuroepithelial bodies in mouse lungs. Histochem Cell Biol. 2008

Carolan BJ, Heguy A, Harvey BG, Leopold PL, Ferris B, Crystal RG. Up-regulation of expression of the ubiquitin carboxyl-terminal hydrolase L1 gene in human airway epithelium of cigarette smokers. Cancer Res 2006;66:10729–10740. [PubMed: 17108109]

DasGupta R, Fuchs E. Multiple roles for activated LEF/TCF transcription complexes during hair follicle development and differentiation. Development 1999;126:4557–4568. [PubMed: 10498690]

De Langhe SP, Carraro G, Tefft D, Li C, Xu X, Chai Y, Minoo P, Hajihosseini MK, Drouin J, Kaartinen V, Bellusci S. Formation and differentiation of multiple mesenchymal lineages during lung development is regulated by beta-catenin signaling. PLoS ONE 2008;3:e1516. [PubMed: 18231602]

Ebert MP, Fei G, Kahmann S, Muller O, Yu J, Sung JJ, Malfertheiner P. Increased beta-catenin mRNA levels and mutational alterations of the APC and beta-catenin gene are present in intestinal-type gastric cancer. Carcinogenesis 2002;23:87–91. [PubMed: 11756228]

Fearnhead NS, Winney B, Bodmer WF. Rare variant hypothesis for multifactorial inheritance: susceptibility to colorectal adenomas as a model. Cell Cycle 2005;4:521–525. [PubMed: 15753653]

Fein AM, Lipschutz JB, Lee CT, Kucich U, Lippmann M, Weinbaum G. COPD and endobronchial polyposis associated with hypogammaglobulinemia. Are proteolytic enzymes involved? Chest 1982;82:127–129. [PubMed: 7083923]

Grigoryan T, Wend P, Klaus A, Birchmeier W. Deciphering the function of canonical Wnt signals in development and disease: conditional loss- and gain-of-function mutations of beta-catenin in mice. Genes Dev 2008;22:2308–2341. [PubMed: 18765787]

Haegel H, Larue L, Ohsugi M, Fedorov L, Herrenknecht K, Kemler R. Lack of beta-catenin affects mouse development at gastrulation. Development 1995;121:3529–3537. [PubMed: 8582267]

Haegele L, Ingold B, Naumann H, Tabatabai G, Ledermann B, Brandner S. Wnt signalling inhibits neural differentiation of embryonic stem cells by controlling bone morphogenetic protein expression. Mol Cell Neurosci 2003;24:696–708. [PubMed: 14664819]

Han G, Li AG, Liang YY, Owens P, He W, Lu S, Yoshimatsu Y, Wang D, Ten Dijke P, Lin X, Wang XJ. Smad7-induced beta-catenin degradation alters epidermal appendage development. Dev Cell 2006;11:301–312. [PubMed: 16950122]

Harada N, Miyoshi H, Murai N, Oshima H, Tamai Y, Oshima M, Taketo MM. Lack of tumorigenesis in the mouse liver after adenovirus-mediated expression of a dominant stable mutant of beta-catenin. Cancer Res 2002;62:1971–1977. [PubMed: 11929813]

Harada N, Tamai Y, Ishikawa T, Sauer B, Takaku K, Oshima M, Taketo MM. Intestinal polyposis in mice with a dominant stable mutation of the beta-catenin gene. EMBO J 1999;18:5931–5942. [PubMed: 10545105]

Hogan BL. Developmental signalling. Sorting out the signals. Curr Biol 1994;4:1122–1124. [PubMed: 7704577]

Hong KU, Reynolds SD, Watkins S, Fuchs E, Stripp BR. Basal cells are a multipotent progenitor capable of renewing the bronchial epithelium. Am J Pathol 2004;164:577–588. [PubMed: 14742263]

Hyatt BA, Shangguan X, Shannon JM. BMP4 modulates fibroblast growth factor-mediated induction of proximal and distal lung differentiation in mouse embryonic tracheal epithelium in mesenchyme-free culture. Dev Dyn 2002;225:153–165. [PubMed: 12242715]

Kemler R, Hierholzer A, Kanzler B, Kuppig S, Hansen K, Taketo MM, de Vries WN, Knowles BB, Solter D. Stabilization of beta-catenin in the mouse zygote leads to premature epithelial-mesenchymal transition in the epiblast. Development 2004;131:5817–5824. [PubMed: 15525667]

Kolligs FT, Nieman MT, Winer I, Hu G, Van Mater D, Feng Y, Smith IM, Wu R, Zhai Y, Cho KR, Fearon ER. ITF-2, a downstream target of the Wnt/TCF pathway, is activated in human cancers with beta-catenin defects and promotes neoplastic transformation. Cancer Cell 2002;1:145–155. [PubMed: 12086873]

Li C, Hu L, Xiao J, Chen H, Li JT, Bellusci S, Delanghe S, Minoo P. Wnt5a regulates Shh and Fgf10 signaling during lung development. Dev Biol 2005;287:86–97. [PubMed: 16169547]

Li C, Xiao J, Hormi K, Borok Z, Minoo P. Wnt5a participates in distal lung morphogenesis. Dev Biol 2002;248:68–81. [PubMed: 12142021]

Li G, Iyengar R. Calpain as an effector of the Gq signaling pathway for inhibition of Wnt/beta-catenin-regulated cell proliferation. Proc Natl Acad Sci U S A 2002;99:13254–13259. [PubMed: 12239346]

Ling L, Nurcombe V, Cool SM. Wnt signaling controls the fate of mesenchymal stem cells. Gene 2009;433:1–7. [PubMed: 19135507]

Liu J, Stevens J, Rote CA, Yost HJ, Hu Y, Neufeld KL, White RL, Matsunami N. Siah-1 mediates a novel beta-catenin degradation pathway linking p53 to the adenomatous polyposis coli protein. Mol Cell 2001;7:927–936. [PubMed: 11389840]

Logan CY, Nusse R. The Wnt signaling pathway in development and disease. Annu Rev Cell Dev Biol 2004;20:781–810. [PubMed: 15473860]

Lu MM, Yang H, Zhang L, Shu W, Blair DG, Morrisey EE. The bone morphogenic protein antagonist gremlin regulates proximal-distal patterning of the lung. Dev Dyn 2001;222:667–680. [PubMed: 11748835]

Marikawa Y, Elinson RP. beta-TrCP is a negative regulator of Wnt/beta-catenin signaling pathway and dorsal axis formation in Xenopus embryos. Mech Dev 1998;77:75–80. [PubMed: 9784611]

Matsuzawa SI, Reed JC. Siah-1, SIP, and Ebi collaborate in a novel pathway for beta-catenin degradation linked to p53 responses. Mol Cell 2001;7:915–926. [PubMed: 11389839]

Morin PJ, Sparks AB, Korinek V, Barker N, Clevers H, Vogelstein B, Kinzler KW. Activation of beta-catenin-Tcf signaling in colon cancer by mutations in beta-catenin or APC. Science 1997;275:1787–1790. [PubMed: 9065402]

Morson B. President's address. The polyp-cancer sequence in the large bowel. Proc R Soc Med 1974;67:451–457. [PubMed: 4853754]

Mucenski ML, Nation JM, Thitoff AR, Besnard V, Xu Y, Wert SE, Harada N, Taketo MM, Stahlman MT, Whitsett JA. Beta-catenin regulates differentiation of respiratory epithelial cells in vivo. Am J Physiol Lung Cell Mol Physiol 2005;289:L971–979. [PubMed: 16040629]

Mucenski ML, Wert SE, Nation JM, Loudy DE, Huelsken J, Birchmeier W, Morrisey EE, Whitsett JA. beta-Catenin is required for specification of proximal/distal cell fate during lung morphogenesis. J Biol Chem 2003;278:40231–40238. [PubMed: 12885771]

Okubo T, Hogan BL. Hyperactive Wnt signaling changes the developmental potential of embryonic lung endoderm. J Biol 2004;3:11. [PubMed: 15186480]

Poulsen TT, Biologist XN, Poulsen HS, Linnoila RI. Acute damage by naphthalene triggers expression of the neuroendocrine marker PGP9.5 in airway epithelial cells. Toxicol Lett. 2008

Rawlins EL, Hogan BL. Epithelial stem cells of the lung: privileged few or opportunities for many? Development 2006;133:2455–2465. [PubMed: 16735479]

Reynolds SD, Zemke AC, Giangreco A, Brockway BL, Teisanu RM, Drake JA, Mariani T, Di PY, Taketo MM, Stripp BR. Conditional stabilization of beta-catenin expands the pool of lung stem cells. Stem Cells 2008;26:1337–1346. [PubMed: 18356571]

Sanes JR, Rubenstein JL, Nicolas JF. Use of a recombinant retrovirus to study post-implantation cell lineage in mouse embryos. EMBO J 1986;5:3133–3142. [PubMed: 3102226]

Shu W, Guttentag S, Wang Z, Andl T, Ballard P, Lu MM, Piccolo S, Birchmeier W, Whitsett JA, Millar SE, Morrisey EE. Wnt/beta-catenin signaling acts upstream of N-myc, BMP4, and FGF signaling to regulate proximal-distal patterning in the lung. Dev Biol 2005;283:226–239. [PubMed: 15907834]

Shu W, Jiang YQ, Lu MM, Morrisey EE. Wnt7b regulates mesenchymal proliferation and vascular development in the lung. Development 2002;129:4831–4842. [PubMed: 12361974]

Topol L, Jiang X, Choi H, Garrett-Beal L, Carolan PJ, Yang Y. Wnt-5a inhibits the canonical Wnt pathway by promoting GSK-3-independent beta-catenin degradation. J Cell Biol 2003;162:899–908. [PubMed: 12952940]

van Amerongen R, Berns A. Knockout mouse models to study Wnt signal transduction. Trends Genet 2006;22:678–689. [PubMed: 17045694]

Wang Z, Shu W, Lu MM, Morrisey EE. Wnt7b activates canonical signaling in epithelial and vascular smooth muscle cells through interactions with Fzd1, Fzd10, and LRP5. Mol Cell Biol 2005;25:5022–5030. [PubMed: 15923619]

Weaver M, Dunn NR, Hogan BL. Bmp4 and Fgf10 play opposing roles during lung bud morphogenesis. Development 2000;127:2695–2704. [PubMed: 10821767]

Weaver M, Yingling JM, Dunn NR, Bellusci S, Hogan BL. Bmp signaling regulates proximal-distal differentiation of endoderm in mouse lung development. Development 1999;126:4005–4015. [PubMed: 10457010]

Xing Y, Li C, Hu L, Tiozzo C, Li M, Chai Y, Bellusci S, Anderson S, Minoo P. Mechanisms of TGFbeta inhibition of LUNG endodermal morphogenesis: the role of TbetaRII, Smads, Nkx2.1 and Pten. Dev Biol 2008;320:340–350. [PubMed: 18602626]

Xu Q, Tam M, Anderson SA. Fate mapping Nkx2.1-lineage cells in the mouse telencephalon. J Comp Neurol 2008;506:16–29. [PubMed: 17990269]

Yamada M, Kuwano K, Maeyama T, Hamada N, Yoshimi M, Nakanishi Y, Kasper M. Dual-immunohistochemistry provides little evidence for epithelial-mesenchymal transition in pulmonary fibrosis. Histochem Cell Biol 2008;129:453–462. [PubMed: 18236067]

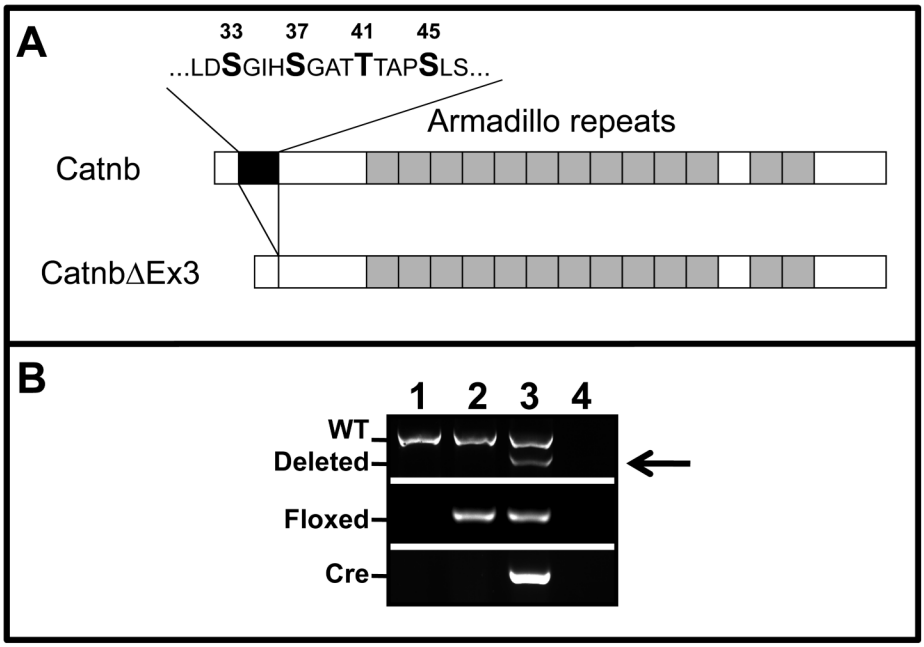

a

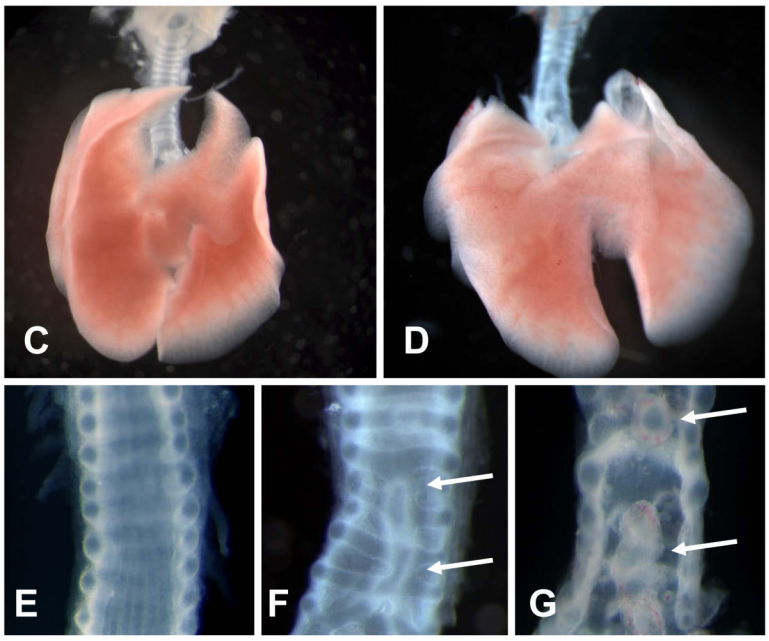

b

c

Figure 1.

Panel A: Schematic illustration of Catnb and CatnbΔEx3 protein structures. 76 amino acids encoded by exon 3 (black box) is deleted in CatnbΔEx3. The deleted region contains phosphorylation sites of CK1 (S45) and GSK3β (S33, S37 and T41). Panel B: Deletion of exon 3 in *CatnbEx3(cko/+)* lung as determined by PCR. Genomic DNA was isolated from lungs of wild-type control (1), *CatnbEx3(f/+)* (2), and *CatnbEx3(cko/+)*(3) embryos and used in PCR analysis. Top panel shows PCR products amplified by CatnbF & CatnbR2 primers. PCR from the wild-type allele results in an 867 bp product, while the exon 3 deletion allele results in a smaller product (arrow). Center panel shows PCR products amplified by CatnbF & CatnbR1 primers. A product of 300 bp was amplified from the exon 3 floxed allele. Bottom panel shows PCR products amplified by cre primers. Lane 4 shows PCR reactions with H2O instead of DNA, and was used as negative control. Panels C and D show whole-mount photo of E18 control (C) and *CatnbEx3(cko/+)* (D) lungs, respectively. High magnification images of control (E) and mutant (F & G) tracheas are shown. Arrows in panel G indicate polyp-like structures along the mutant trachea. Comparison of the control (left) and mutant (right) lung lobes were shown in panels H to L. Scale bar: 1 mm(C, D, H-L); 250 um (E-G).

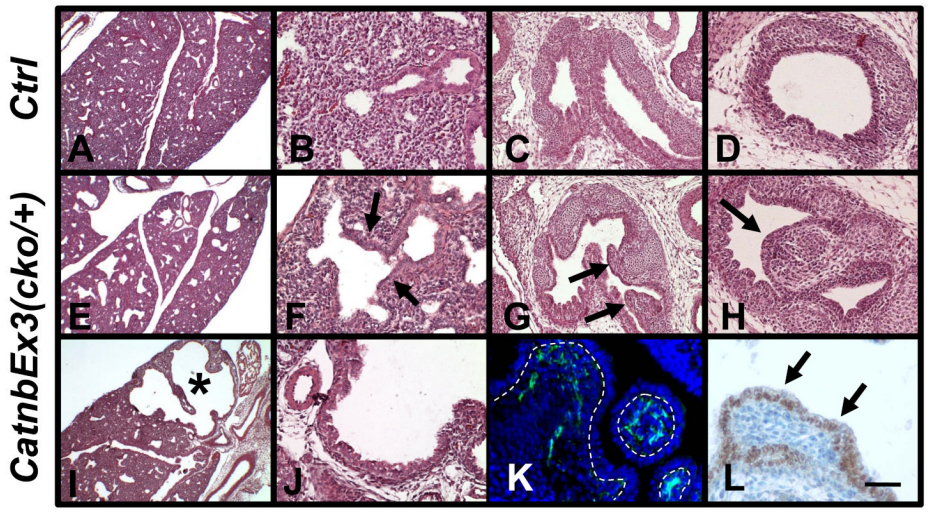

Figure 2.

H&E staining of E16 control (A to D) and *CatnbEx3(cko/+)* (E to J) lungs. Arrows in F indicate dilation of primitive bronchial-alveolar duct junction in mutant lung. Asterisk in panel I indicates a severely dilated area in the mutant lung. Frontal plans of main-stem bronchi are shown in panels C and G. Arrows in G indicate polyp structures in the mutant main-stem bronchi. Trachea sections of control and mutant are shown in panels D and H, respectively. Arrow in H indicates polyp structures in the mutant trachea.

Mesenchymal cells of the polyps were labeled by immunostaining with vimentin antibody (green, K) and the epithelial cells (arrows, L) were labeled by Nkx2.1 antibody. Doted lines in panel K indicate epithelial-mesenchymal adjunctions. Morphology of the tissue in panel K was shown by DAPI-staining. Scale bar: 400 um (A, E, I); 80 um (B, D, F, H, J); 120 um (C, G); 40 um (K, L).

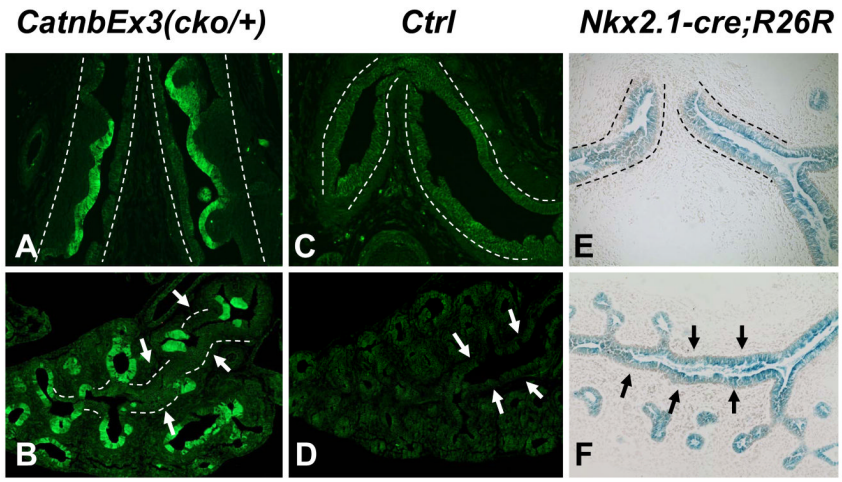

a

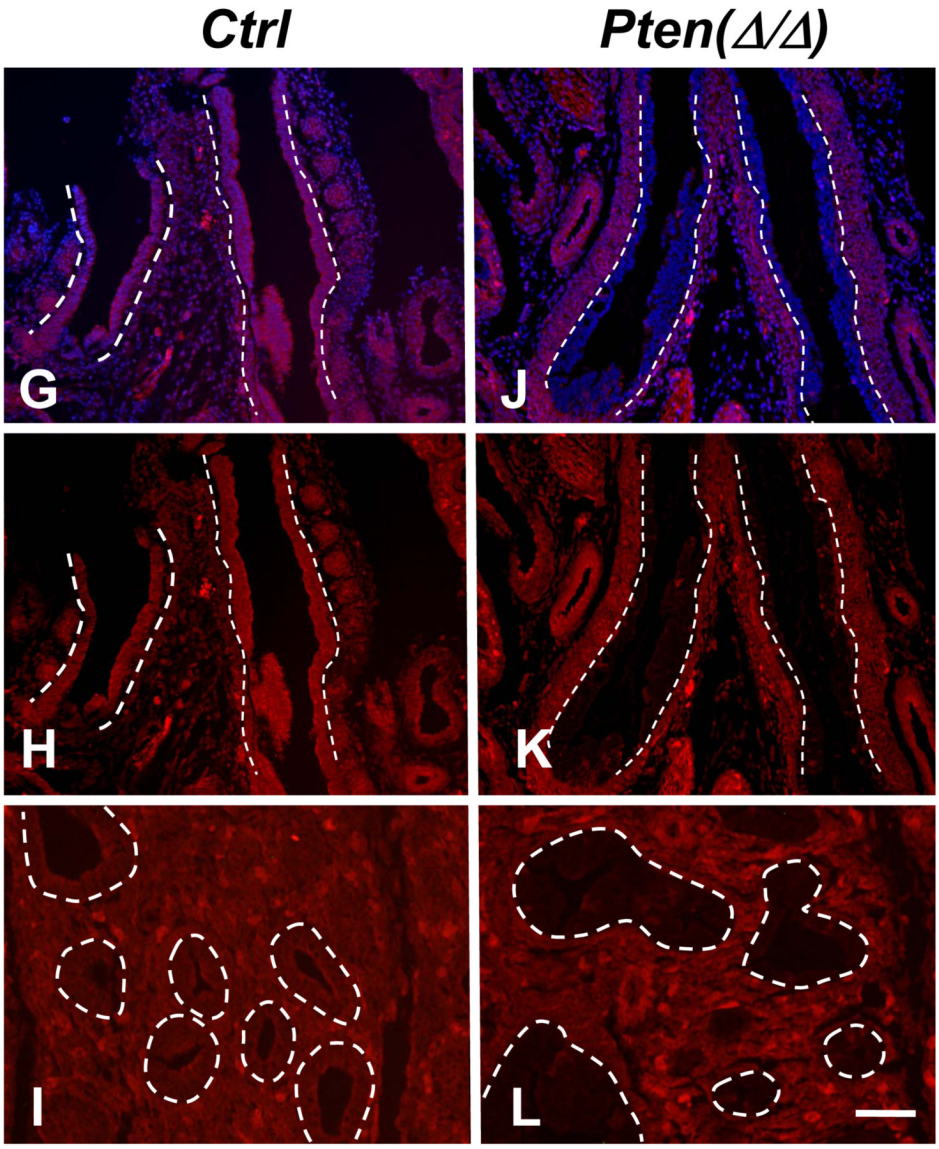

b

Figure 3.

Immunofluorescent staining for β-catenin (A to D) in E14 control (C & D) and *CatnbEx3 (cko/+)* (A & B) main-stem bronchi (MSB) and lungs. Panels A, C and E are frontal plans of MSB. Doted lines in panels A, C and E outline the airway of MSBs. Note β-catenin is present in both sides of MSB in the wild type lung (Green in C), but β-catenin accumulates preferentially in the outer wall epithelium of the mutant MSB (Bright Green in A). Panels E & F show LacZ staining in *Nkx2.1-cre; R26R-LacZ* MSB and lung, respectively. Immunofluorescent staining for Pten in E14 control (G to I) and *Nkx2.1-cre; Pten(f/f)* [*Pten (Δ/Δ)*, J to L] MSB and distal lungs. Frontal plans of MSB are shown. Doted lines indicate the adjunction between epithelium and mesenchyme of MSB (G, H, J, and K) and distal lung (I and L). Note Pten is uniformly expressed in the epithelial cells of control MSB and distal lung but is not detectable in epithelial cells of *Nkx2.1-cre; Pten(f/f)* MSB (J & K) and distal lung (L). Panels G & J were counterstained with DAPI. Scale bar: 80 um.

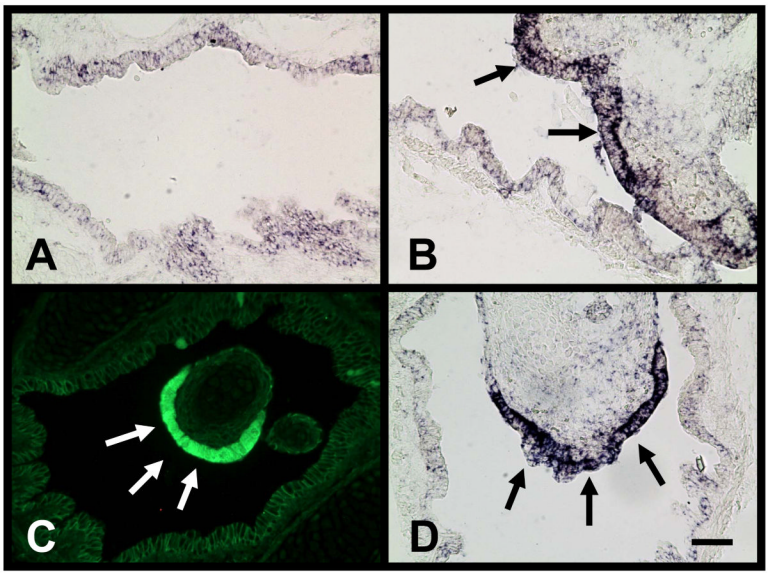

Figure 4.

In situ hybridization for β-catenin mRNA (A, B & D) in E18 control (A) and *CatnbEx3(cko/+)* (B & D) proximal airways. Moderate levels of β-catenin mRNA were detected in control MSB (A). Arrows indicate increased β-catenin mRNA levels in polyp epithelial cells found in the mutant MSB (B) and Trachea (D). Please note striking spatial overlap between increased β-catenin mRNA (D) and protein accumulation as determined by Immunofluorescent staining (C) in mutant lungs. Scale bar: 40 um.

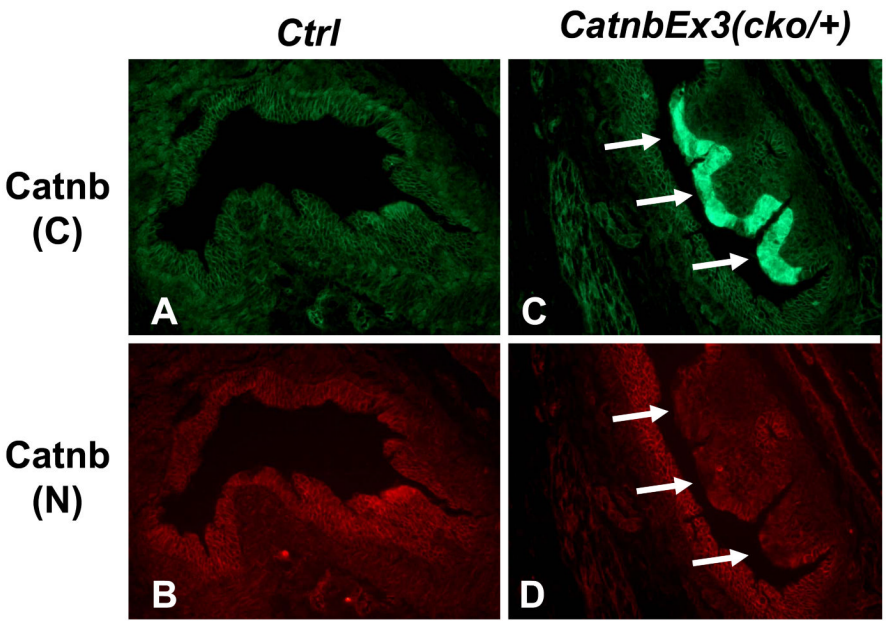

a

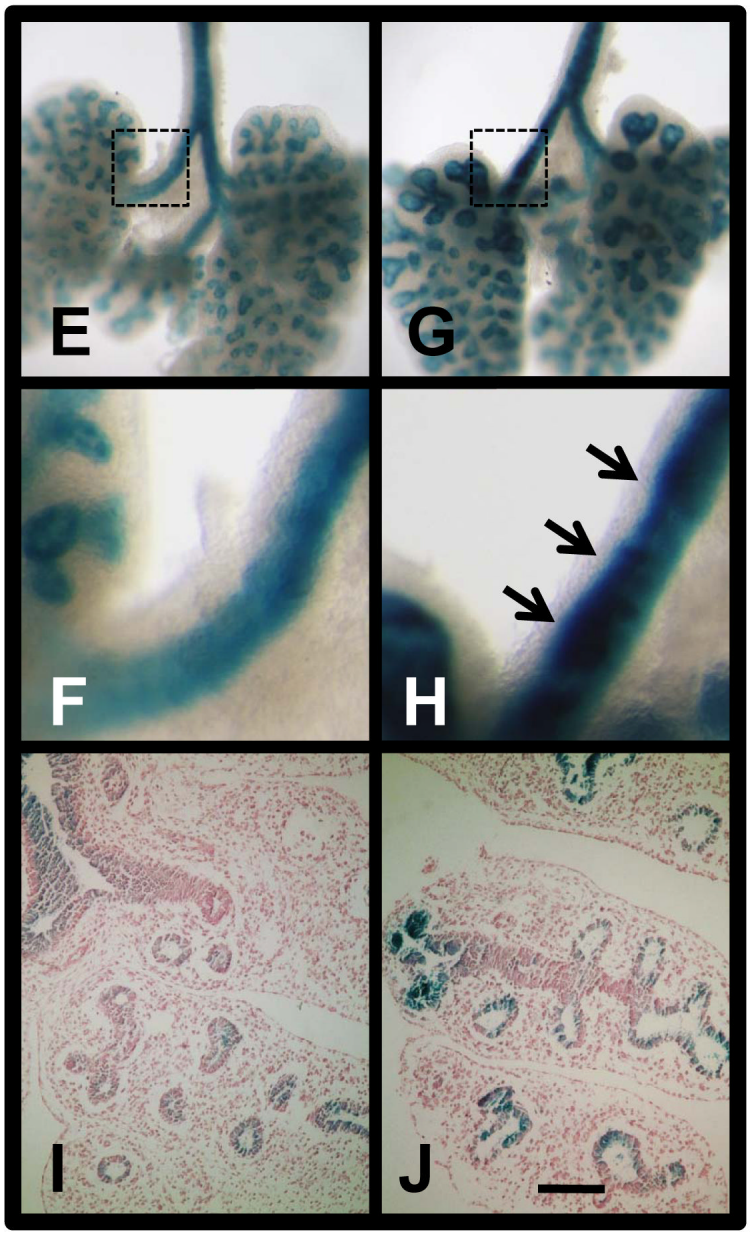

b

Figure 5.

Immunofluorescent staining of E14 control (A & B) and *CatnbEx3(cko/+)* (C & D) main-stem bronchi (MSB) with antibodies against β-catenin (C terminal, green) and β-catenin (N terminal, "wild type" red). Arrows indicate the polyps.

LacZ staining of E13 TOPGAL (E & F) and *Nkx2.1-cre;Catnb[+/lox(ex3)];TOPGAL (*G & H*)* lungs from siblings. F & H are higher magnification of boxed areas of E & G, respectively. I & J are sections of stained TOPGAL and *Nkx2.1-cre;Catnb[+/lox(ex3)];TOPGAL* lungs with eosin counter staining, respectively. Scale bar: 40 um (A-D); 1 mm (E, G); 250 um (F, H); 120 um (I, J).

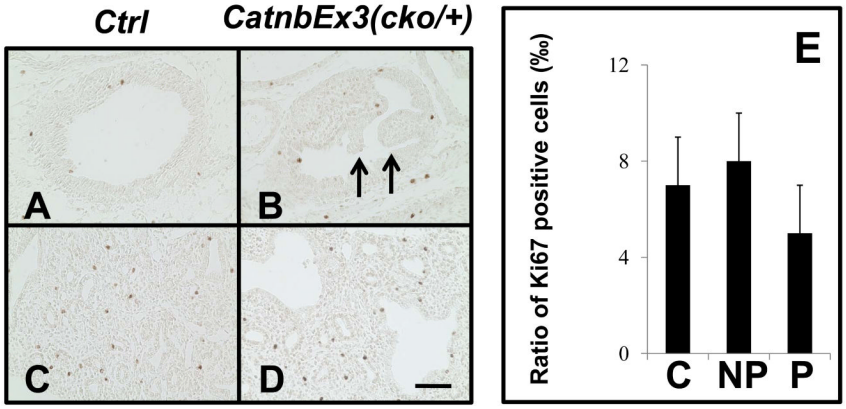

Figure 6.

Proliferation in E15 control (A, C) and *CatnbEx3(cko/+)* (B, D) lungs determined by immunostaining with Ki67 antibody. Arrows indicate polyps formed along proximal airways. Panel E indicates ratio of proliferating epithelial cells in the control (C) proximal airways, the none-polyp areas (NP) and the polyps (P) of mutant proximal airways. No statistically significant difference was observed between ratios of "C" and "NP" or "C" and "P". Scale bar: 80 um.

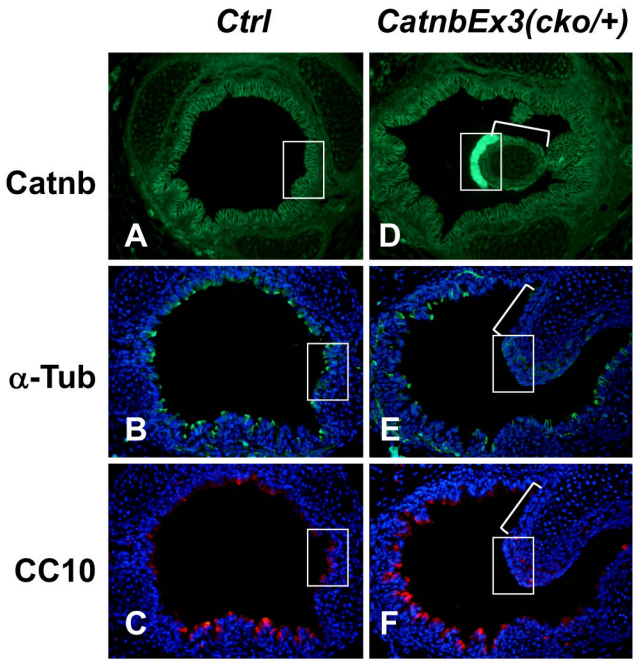

a

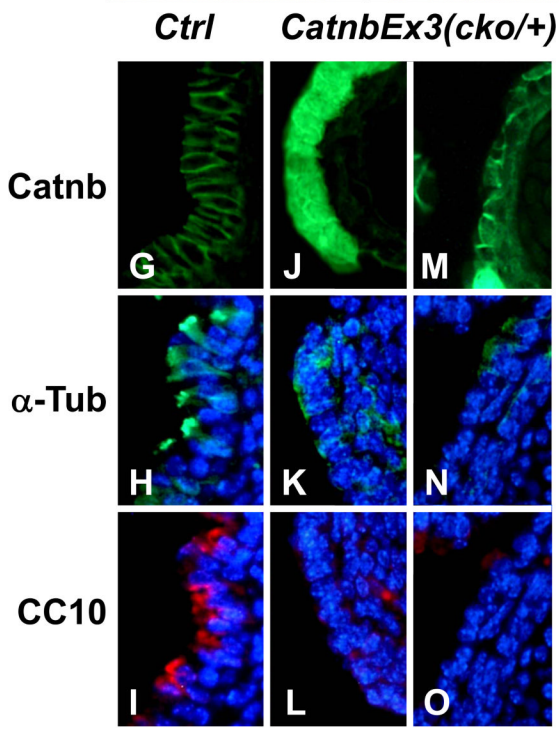

b

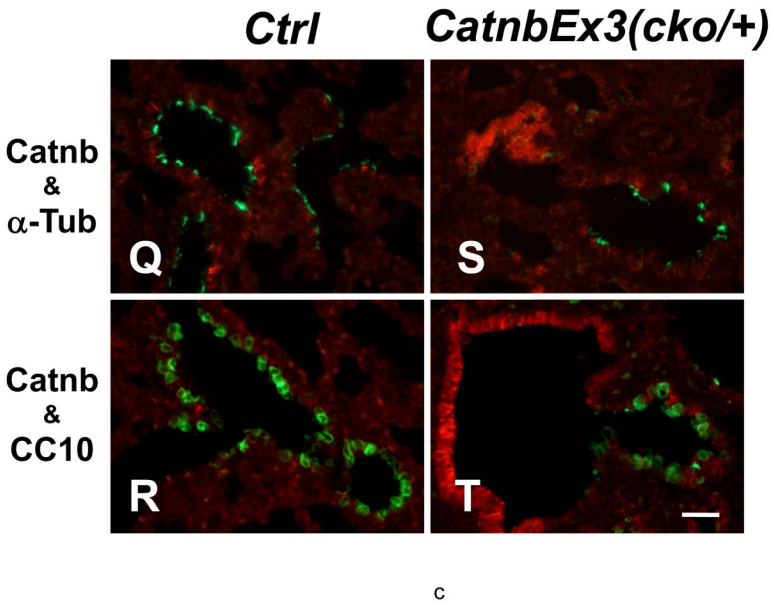

c

Figure 7.

Immunofluorescent staining of E18 control (A-C, G-I, Q-R) and *CatnbEx3(cko/+)* (D-F, J-O, S-T) trachea and lung with antibodies against α-tubulin (B, E, H, K, N, Q & S; green) and CC10 (C, F, I, L & O, red; R & T, green). High magnifications of boxed areas in panels A to F are shown in panels G to L, respectively. High magnifications of bracket areas in panels D to F are shown in panels M to O, respectively. Panels Q and S show double-staining of α-tubulin (green) and β-catenin (red) in control and mutant bronchioles, respectively. Panels R and T show double-staining of CC10 (green) and β-catenin (red) in control and mutant bronchioles, respectively. Scale bar: 80 um (A-F); 20 um (G-O); 40 um (Q-T).

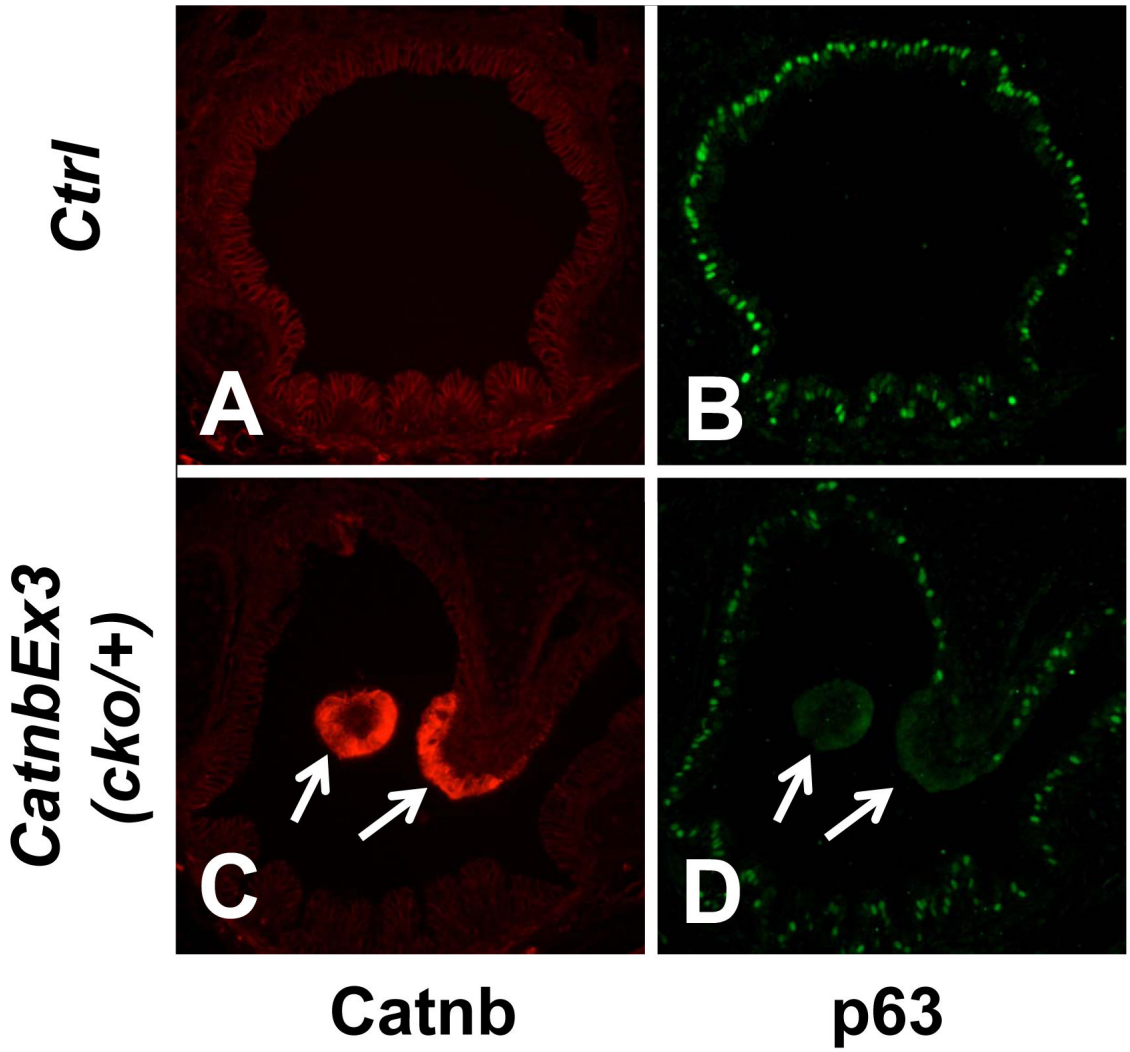

a

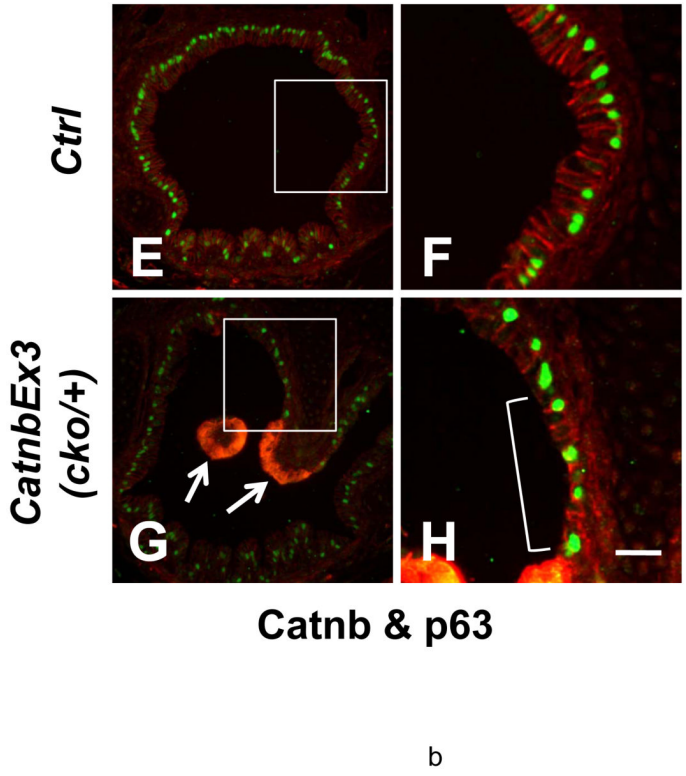

b

Figure 8.

Immunofluorescent staining of E18 control (A, B, E & F) and *CatnbEx3(cko/+)* (C, D, G & H) trachea with antibodies against p63 (green) and β-catenin (red). Arrows indicate absence of p63 and accumulation of β-catenin in epithelial cells at apical surface of tracheal polyps. Note that the p63 positive cells were covered with a layer of columnar epithelial cells in control trachea (F), whereas the p63 positive cells were exposed directly to the lumen of the trachea (bracket, H) in the epithelium adjacent to cells with accumulated β-catenin. Scale bar: 80 um (A-E, G); 30 um (F, H).

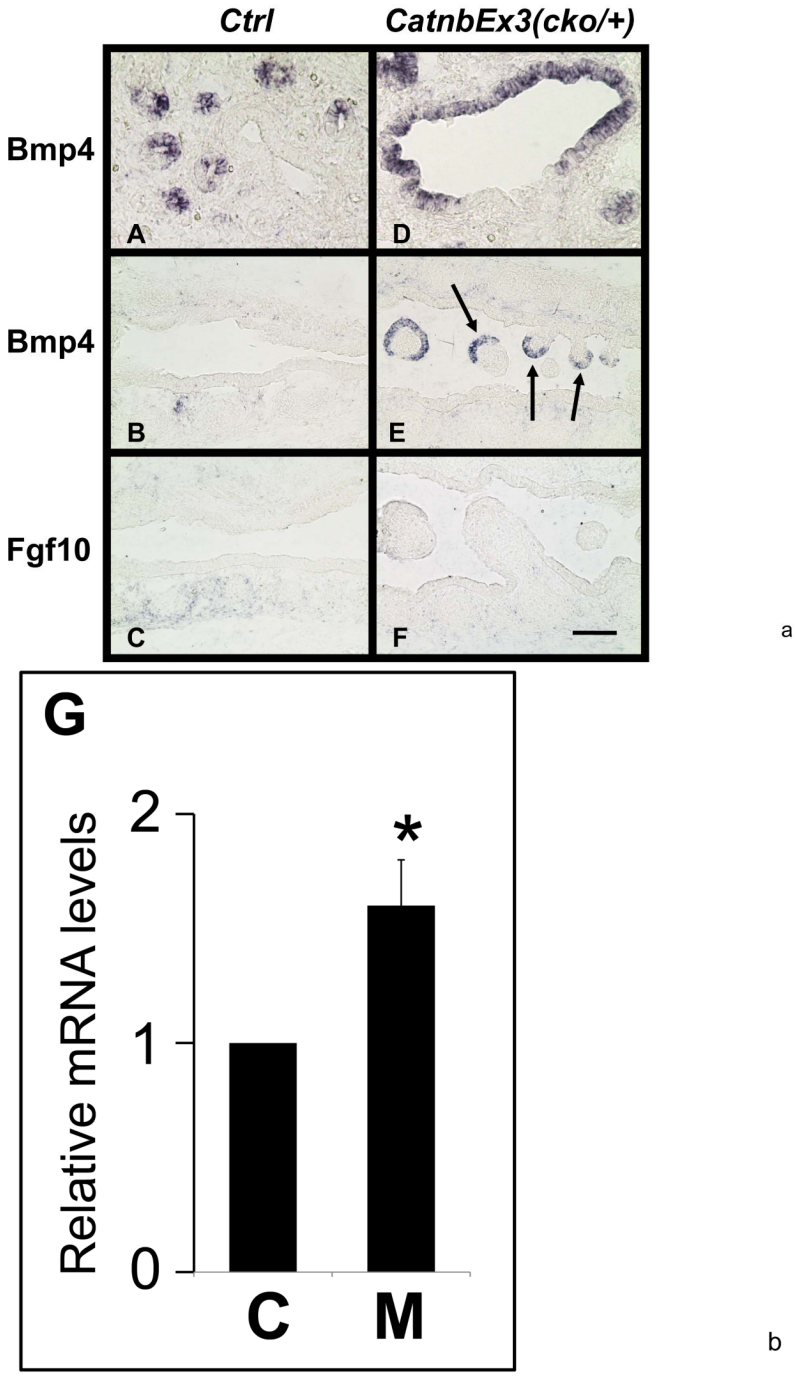

Figure 9.

In situ hybridization for Bmp4 and Fgf10 mRNA in E15 control (A to C) and *CatnbEx3(cko/+)* (D to F) lungs and trachea. Bmp4 was nearly undetectable in control trachea (B). Arrows in panel E indicate induction of high Bmp4 levels in polyp epithelial cells in mutant trachea. Scale bar: 40 um (A, D); 80 um (B, C, E, F).

Panel G. Relative mRNA levels of Bmp4 in mutant (M) vs. control lungs (C) by quantitative RT-PCR. Levels of mRNA were normalized to that of TATA Binding Protein (TBP). * indicates $P<0.05$.

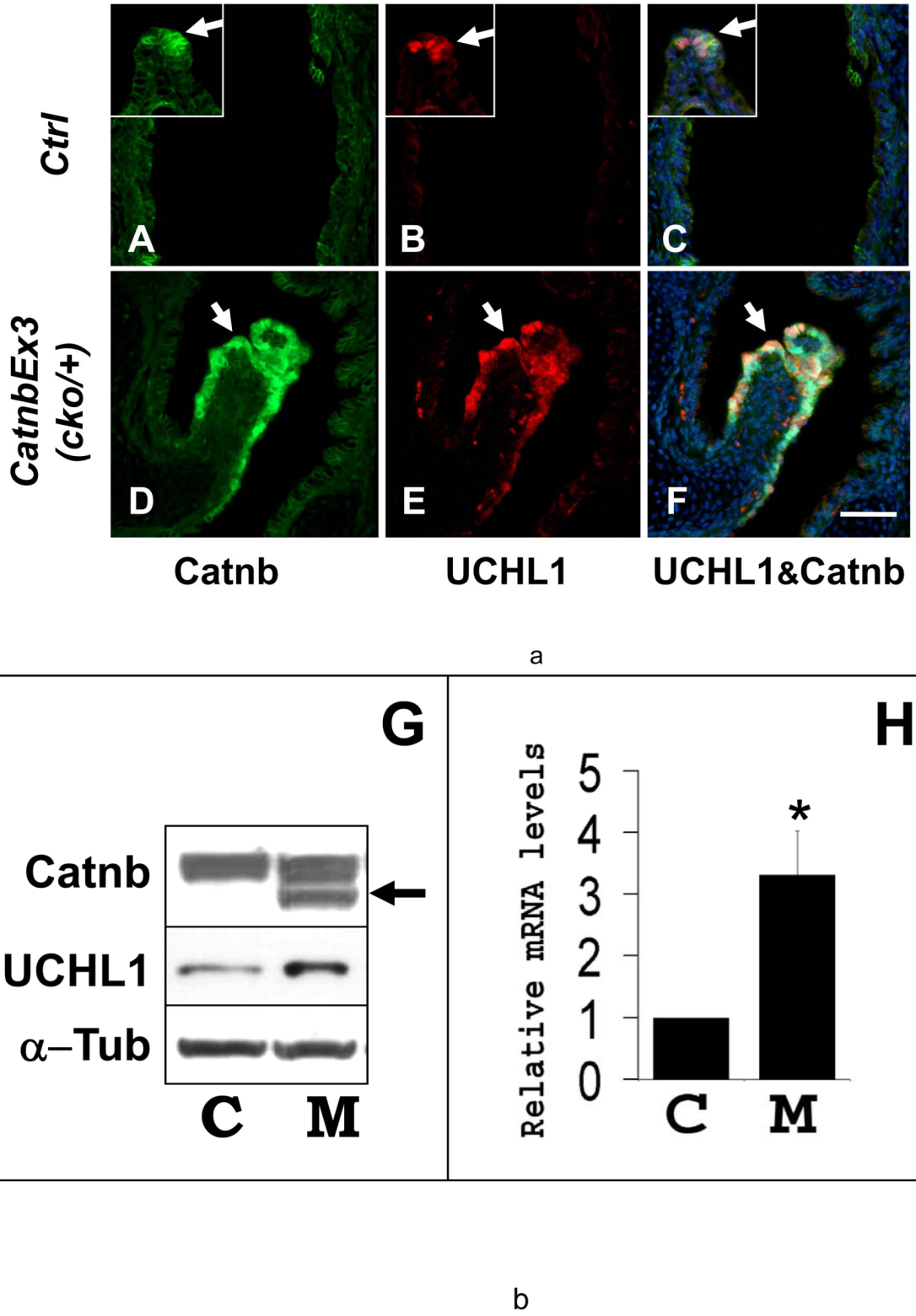

Figure 10.

Immunofluorescent staining of control E18 (A to C) and *CatnbEx3(cko/+)* (D to F) trachea with antibodies against β-catenin (A & D; green) and UCHL1 (B & E; red). Insets in panels A

to C show staining on NEB in control lungs. Panels C & F show merged image of A & B and D & E, respectively, with DAPI-labeled nuclei. Scale bar: 80 um.

Panel G. Western blot analysis of control (C) and *CatnbEx3(cko/+)* (M) lungs for protein levels of β-catenin and UCHL1. Arrow indicates truncated β-catenin. Similar amount of total proteins were loaded as indicated by levels of α-tubulin.

Panel H. Relative mRNA levels of UCHL1 in control (C) vs. mutant (M) lungs by quantitative RT-PCR. mRNA levels were normalized to that of TATA binding protein (TBP). * indicates $P<0.05$.

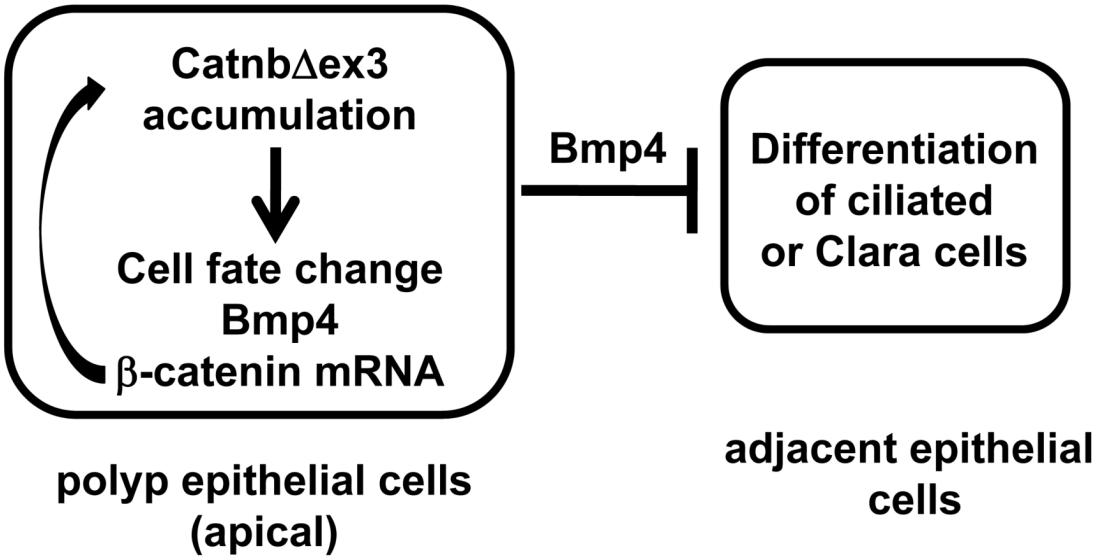

Figure 11.

A simplistic schematic model of mechanisms related to β-catenin accumulation. In apical epithelial cells of the polyps, accumulation of β-catenin results in cell fate changes associated with increased expression of Bmp4 and β-catenin. High levels of Bmp4 thereby regulate differentiation of the adjacent epithelial cells lining the stalk of the polyps.